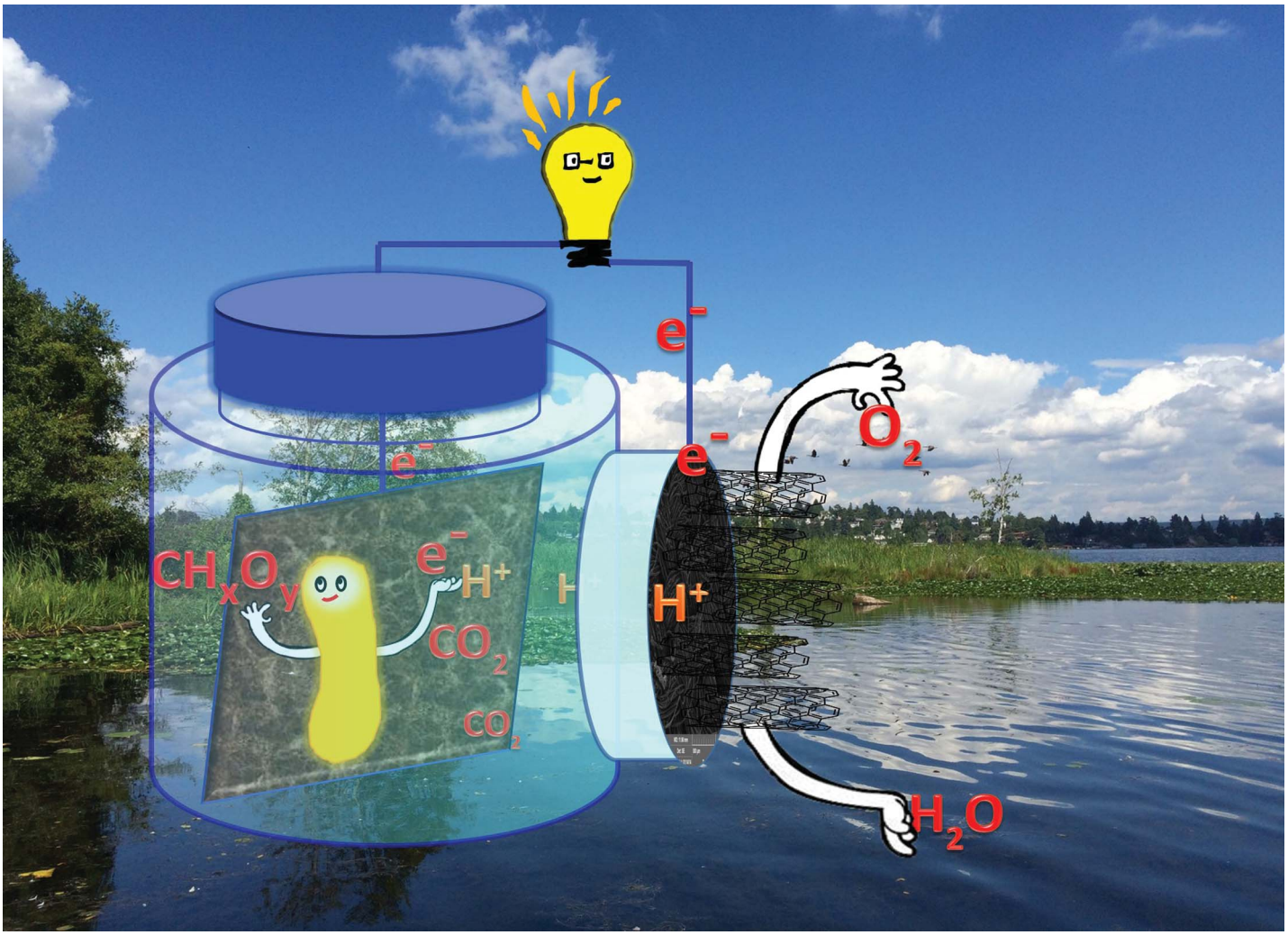

Showcasing the study on novel vertically aligned nitrogen-doped carbon nanotubes used as the cathode of a microbial fuel cell by Prof. Han-Qing Yu at CAS Key Laboratory of Urban Pollutant Conversion, Department of Chemistry, University of Science and Technology of China, and Dr Li-Ming Dai at Department of Macromolecular Science and Engineering, Case Western Reserve University.

Title: Preparation of microvillus-like nitrogen-doped carbon nanotubes as the cathode of a microbial fuel cell

Microbial fuel cells (MFCs) generally suffer from poor cathode performance. To improve this, a novel cathode material was prepared by growing vertically aligned nitrogen-doped carbon nanotubes on carbon cloth, offering an efficient, metal-free, and low-cost cathode for MFCs.

As featured in:

See Li-Ming Dai, Han-Qing Yu *et al.*, *J. Mater. Chem. A*, 2016, **4**, 1632.

ROYAL SOCIETY OF CHEMISTRY

www.rsc.org/MaterialsA

Registered charity number: 207890

Journal of Materials Chemistry A

PAPER

View Article Online
View Journal | View Issue

Cite this: J. Mater. Chem. A, 2016, 4, 1632

Preparation of microvillus-like nitrogen-doped carbon nanotubes as the cathode of a microbial fuel cell†

Yan-Rong He,[ab] Feng Du,[b] Yu-Xi Huang,[a] Li-Ming Dai,*[b] Wen-Wei Li[a] and Han-Qing Yu*[a]

Received 24th August 2015
Accepted 11th November 2015

DOI: 10.1039/c5ta06673e

www.rsc.org/MaterialsA

A microbial fuel cell (MFC) is an emerging technology to harvest electricity from waste, but generally suffers from low power density at the present stage. Especially, the poor cathode performance usually presents a limiting factor. In this work, we prepare a novel cathode material for an MFC by growing vertically-aligned nitrogen-doped carbon nanotubes (N-CNTs) on carbon cloth (CC) using a chemical vapor deposition method, and evaluate its performance in MFC tests. The results show that the MFC with the N-CNT–CC as its cathode exhibits an output power density of 542 mW m^{-3}, greater than that of the MFC with the Pt/C-coated CC cathode. The electrochemical experimental results show higher catalytic activity for oxygen reduction and a smaller resistance of the N-CNT–CC electrode, compared to those of the Pt/C-CC, which are responsible for its better MFC performance. The N-CNT–CC material prepared in this work may offer an appealing metal-free and low-cost alternative to Pt/C for MFC cathode applications.

A microbial fuel cell (MFC) is an emerging technology to produce electricity directly from waste streams.[1–4] In an MFC anode, the electrons released from the metabolism of organic matters are transferred to the anode and ultimately reduced at the cathode. Various oxidants such as ferricyanide,[5] permanganate,[6] and oxygen,[7] can be used as electron acceptors at the cathode. Especially, oxygen as an abundant and freely-available electron acceptor has been most widely adopted.[8] Although MFCs have unique advantages, they have not yet been put to practical application because of their low power generation and high costs. One common limitation in energy production from MFCs is the considerable overpotential of the oxygen-reducing cathode.[9]

Platinum (Pt)/carbon (C) is the most widely used catalyst for oxygen reduction reaction (ORR) at an MFC cathode due to its high catalytic activity, but the high cost and limited availability constraints its practical application.[10] Half of the capital cost of an MFC comes from the cathode if Pt/C is used.[9] Apart from its high cost, a Pt-based catalyst also suffers from unstable performance. Therefore, to reduce MFC costs and make it sustainable for commercial applications, it is highly desired to develop effective and low-cost catalysts to replace Pt/C.

Metal-free carbon materials, owing to their low cost and wide availability, have been extensively investigated as ORR catalysts.[11–15] In particular, carbon nanotubes (CNTs) are regarded as a highly-efficient ORR catalyst, attributed to their high surface area, electrocatalytic activity, corrosion resistance, and excellent conductivity. Furthermore, compared to Pt, which gets easily poisoned, CNT is a robust catalyst used in polluted environments. Moreover, heteroatom doping is usually applied to further improve its ORR performance.[16–18] For instance, nitrogen-doped CNTs exhibit a similar or even higher catalytic activity and better stability as well as excellent tolerance to methanol and CO compared to Pt-based catalysts when Pt is poisoned.[19–21] CNT-modified air cathodes have been previously manufactured using coating methods.[22,23] In other studies, vertically-aligned CNT electrodes were also prepared, which exhibited even better electrochemical performance attributed to their unique electrical, mechanical, thermal and conductive properties.[24,25] However, no application of such vertically-aligned CNT electrodes for MFC cathodes has been reported.

In this work, we prepared a vertically-aligned, nitrogen-doped CNT (N-CNT)–carbon cloth (CC) composite electrode by growing N-CNTs on CC using a chemical vapor deposition (CVD) method and used it as an MFC cathode. Then, we compared the performance of MFCs with this N-CNT–CC cathode and a traditional Pt/CC cathode, characterized their electrochemical properties and explored the reason for the better performance of the MFC with the N-CNT–CC cathode.

[a]CAS Key Laboratory of Urban Pollutant Conversion, Department of Chemistry, University of Science & Technology of China, Hefei 230026, China. E-mail: hqyu@ustc.edu.cn

[b]Department of Macromolecular Science and Engineering, Case Western Reserve University, Cleveland, Ohio 44106, USA. E-mail: liming.dai@case.edu

† Electronic supplementary information (ESI) available. See DOI: 10.1039/c5ta06673e

Aligned N-CNTs were prepared directly on the entire CC, which is a conductive sheet of carbon fibers. The SEM images show that N-CNTs were uniformly distributed over the CC surface, forming a three dimensional network structure (Fig. 1a–c). Additionally, the carbon fibers were covered by a 3 μm thick CNT layer, where the CNTs were vertically aligned along carbon fibers. This structure was expected to increase the accessibility of the electrolyte and oxygen to the N-CNTs, and thus improve the mass transfer and benefit the electrochemical reactions.[26]

Fig. 1d shows the Raman spectra of the raw CC, N-CNT–CC, and N-CNTs grown on silicon wafer as a comparison. The D-band and G-band exist in all the electrodes. The D-band is attributed to the A_{1g} phonon of sp^3 carbon atoms of disordered graphite, and the G-band comes from the in-plane vibration of sp^2 carbon atoms.[27] The G-band of the carbon cloth was located at 1583 cm^{-1}, while that of the N-CNT–CC blue-shifted to 1587 cm^{-1},which was close to the value of the N-CNT-silicon wafer (1593 cm^{-1}), indicating the covering of N-CNTs on the carbon cloth. The full width half-maxima of the D-band could be used to evaluate the crystalline structures of the carbon.[28] The full width half-maxima of the raw carbon cloth was 49.1 cm^{-1}, while those of the N-CNT–CC and N-CNT–silicon wafer were 70.0 cm^{-1} and 93.2 cm^{-1}, respectively. This suggests that, after the growth of the N-CNT, the disorderliness on the surface of the electrode increased. This could be attributed to the fact that the CNTs have defects, and in addition, the doping of N elements further disordered the carbon structure of the CNTs. Briefly, after the growth of N-CNTs, the surface of the carbon cloth was covered and the surface properties were also changed.

X-ray photoelectron spectroscopy (XPS) was used to examine the elemental composition and valence state of the N-CNT–CC electrode. The XPS survey spectrum in Fig. 2a shows the C 1s, N 1s, and O 1s with an associated Auger peak. The O peaks might arise from the incorporation of physico-chemically adsorbed oxygen, which was reported to be advantageous for the ORR application.[29] Fig. 2b and c show the core level spectra of C 1s and N 1s, respectively. The main component peak in C 1s at 284.5 eV indicates that graphite carbon was the major component in the N-CNTs,[30] while the peak that appeared at 285.4 eV was attributed to the C–N bond.[31] From the core level N 1s spectra, pyridinic-N and pyrrolic-N located near 398.7 eV and 400.7 eV, respectively, were attributed to C–N sp^3 and C=N sp^2, respectively.[32,33] These results indicate that the well-maintained graphite carbon and the doping of the N might lead to a change of conductivity and ORR activity.

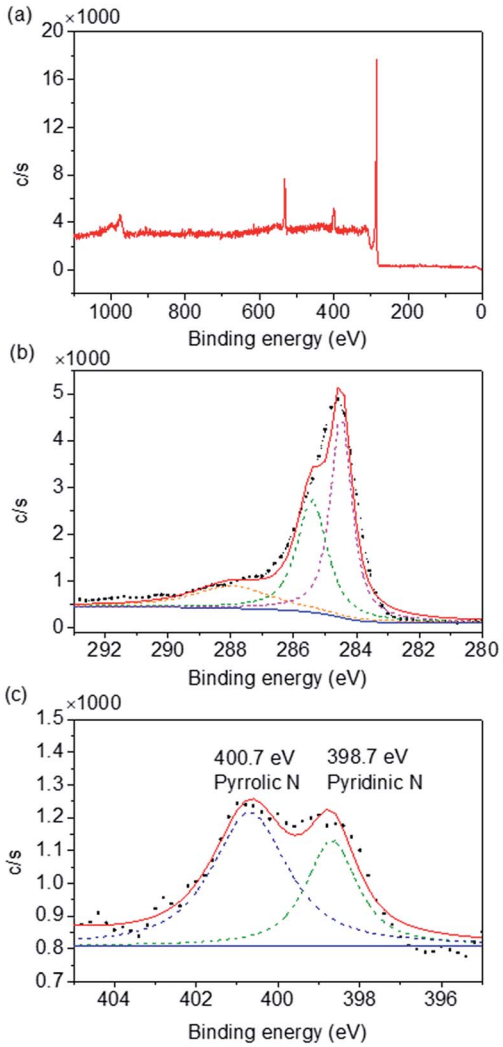

Fig. 2 (a) Sum XPS spectra, and (b) XPS N 1s spectra of the N-CNT–CC electrode.

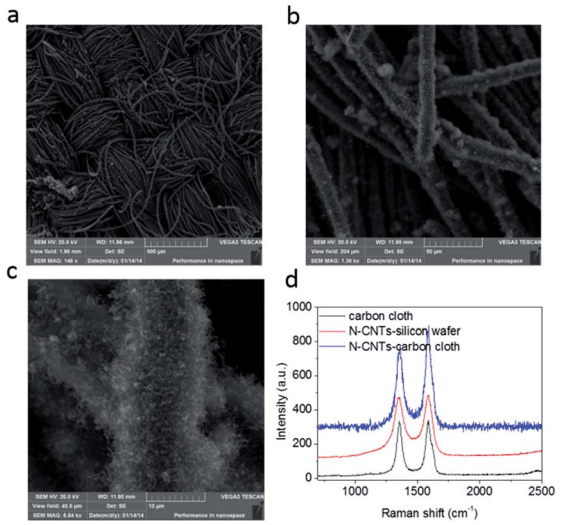

Fig. 1 (a–c) SEM images of the N-CNT–CC electrode; and (d) Raman spectra of the raw CC, N-CNTs on a silicon wafer, and N-CNTs on CC.

The electrocatalytic activity of the N-CNT–CC as an MFC cathode was examined and compared with that of the Pt/C-CC cathode. All the experiments were conducted in duplicate (Fig. 3). Fig. 3a illustrates the output voltages of the MFCs during four cycles. Although the voltages increased gradually over the cycles in both MFCs, the voltages of the N-CNT–CC were in general a little higher than those of the Pt/C-CC. The output voltage of an MFC depends mainly on the potential difference between the anode and the cathode. After the four

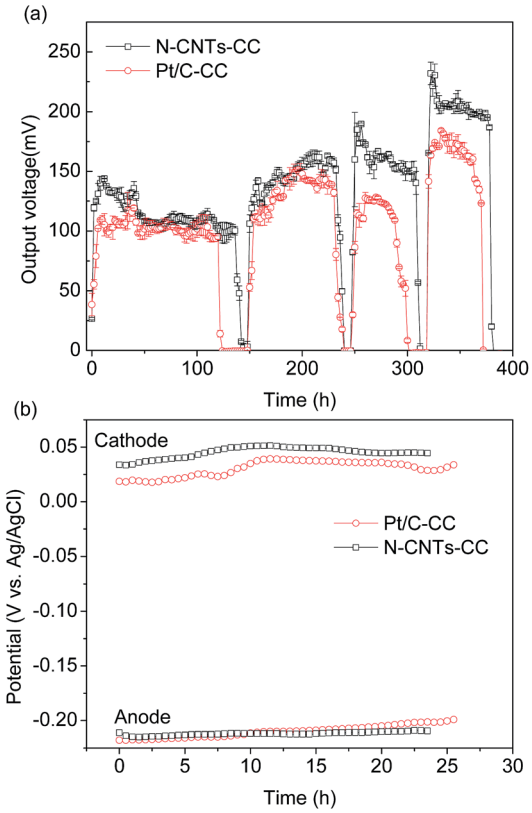

Fig. 3 (a) Output voltage of the MFCs; and (b) anode and cathode potentials of the MFCs with the N-CNT–CC cathode and Pt/C-CC cathode, respectively.

operating cycles, both the anode and cathode potentials of the two MFCs were measured. Fig. 3b shows that the N-CNT–CC has a slightly higher cathode potential, but its anode potential was close to that of Pt/C-CC.

To get a better insight into the electricity generation performance of the two electrodes, the polarization curves and power density curves were measured (Fig. 4). A typical polarization curve shows three different zones, *i.e.*, activation, ohmic and concentration losses.[34] The activation loss shows the proportion of voltage loss occuring in electrode reactions that transfer electrons to/from the electrode. The ohmic loss is mainly originated from the resistance of electron transfer across the electrodes, bacterial biofilm, electrolyte, and proton exchange membrane. The concentration loss is caused by the change in concentration of the reactants at the surface of the electrodes. The polarization curve of the N-CNT–CC showed an almost linear increase of current with decreased voltage, indicating that the voltage loss was dominated by the ohmic loss. In comparison, the Pt/C-CC showed both activation and ohmic loss regions in the polarization curve with a larger slope, suggesting relatively poor ORR activity and a higher internal resistance of the MFC with the Pt/C-CC cathode.[34] The maximum power density of the MFC with the N-CNT–CC reached 542 mW m^{-3} (135 mW m^{-2}), greater than that with the Pt/C-CC (499 mW m^{-3}) by 8.6%. This value is comparable to that reported in a previous study (139 mW m^{-2}),[35] where CNT/Pt composites were used as the MFC cathode, suggesting good ORR catalytic performance of the N-CNT–CC electrode.

The MFC performance is affected by many factors, including reactor configuration, overpotential, and internal resistance.[6] Herein, the ORR catalytic activities of the cathode were examined. The Tafel plots of the N-CNT–CC and Pt/C-CC electrodes are shown in Fig. 5a. Evaluation of the intrinsic electrocatalytic activities of electrocatalysts was made based on the relative values of the exchange current density j_0 for ORR, which is an important kinetic parameter representing the electrochemical reaction at equilibrium.[36] This value is recognized as an indicator of the electron transfer rate of a catalyst, and its

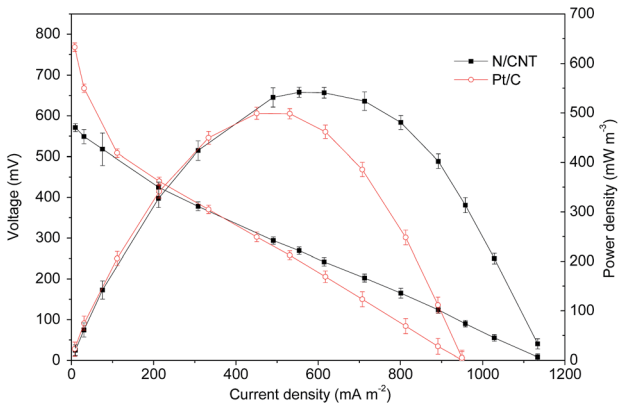

Fig. 4 Polarization curves and power density curves of the MFCs with different cathodes. Black line: N-CNT–CC; red line: Pt/C-CC.

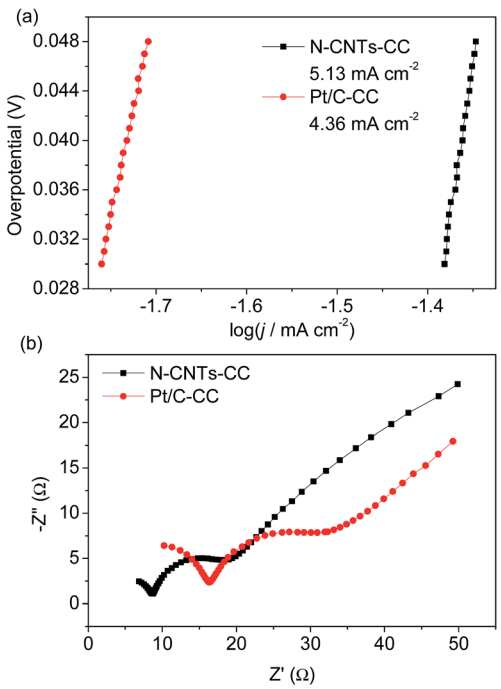

Fig. 5 (a) Tafel plots of the Pt/CC-cathode and N-CNT-cathode recorded in 50 mM phosphate buffer solution of pH 7.0, at the scan rate of 1 mV s^{-1}, and overpotentials from 60 to 80 mV; (b) EIS of the N-CNT–CC and Pt/C-CC electrodes.

magnitude governs how rapidly the electrochemical reaction can occur. In this study, the exchange current density j_0 values were 5.13 mA cm^{-2} and 4.36 mA cm^{-2} for the N-CNT–CC and Pt/C-CC, respectively, indicating that the N-CNT–CC had higher ORR activity.

Electrochemical impedance spectroscopy (EIS) was used to determine the resistance of the cathode reaction (Fig. 5b). By fitting the data of the Nyquist plots, the value of each parameter was obtained. The ohmic loss, R_s resulting from the ionic resistance of the electrolyte, the intrinsic resistance of active materials, and the contact resistance were found to be 9.22 Ω and 16.95 Ω for the N-CNT–CC and Pt/C-CC, respectively. Since both MFCs were operated under exactly the same conditions, the difference in the ohmic resistance should be attributed to the higher conductivity of the CNTs. The activation loss (R_{ct}) of the N-CNT–CC was 11.23 Ω, which was also smaller than 16.30 Ω for the Pt/C-CC, suggesting that the activation energy required to transfer an electron from the N-CNT–CC to the electrolyte was less than that of the Pt/CC. Both the ohmic loss and activation loss of the N-CNT–CC were smaller than those of the Pt/C-CC electrode, which are in good agreement with the Tafel results. The smaller ohmic resistance of the N-CNT–CC electrode might have resulted from the good conductivity of the CNT-CC and the doping of the N element. The core-level spectra of the C 1s in Fig. 2b show that the major component in the CNTs was graphite carbon, which maintained the graphite structure and the conductivity of the CNTs. In addition, a previous study has demonstrated that the doping of graphite-like sp^2 N in a graphite structure could act as a weak electron donor and increase the electrical conductivity of the electrode greatly.[32] In the N-CNT–CC electrode, sp^2 N accounted for a large part of the doped-N in the CNT (Fig. 2c), which would lead to a smaller resistance of the electrode.[19,37] The Warburg resistances of the N-CNT–CC and the Pt/C-CC were 0.011 Ω and 0.0074 Ω, respectively, which were much less than the ohmic loss and the activation loss, indicating that the concentration loss of the MFC system did not play a major role under our experimental conditions.

CV analysis was performed to further evaluate the ORR performance of the two cathodes in 50 mM PBS saturated with oxygen. The two electrodes had the same levels of onset potential, while the cathodic peak potential of the N-CNT–CC was 0.056 V *vs.* Ag/AgCl, which is more positive than that of the Pt/C-CC (Fig. 6). The improved ORR activity of the N-CNT–CC might have resulted from the doped-N defect, which makes the C atoms adjacent to N dopants have a substantially high positive charge density to counterbalance the strong electronic affinity of N.[19] The resulting C atoms could serve as adsorption sites for oxygen and also facilitate charge-transfer at the electrode/electrolyte interface.[38] Although the two electrodes had the same onset potential for ORR, the more positive cathodic peak potential of the N-CNT–CC suggests better catalytic activity of this electrode for ORR.[7] This result is consistent with the above Tafel measurement results.

Several factors, such as conductivity, catalytic activity for ORR, hydrophobicity, might contribute to the enhanced cathode performance of the N-CNT–CC electrode. The EIS

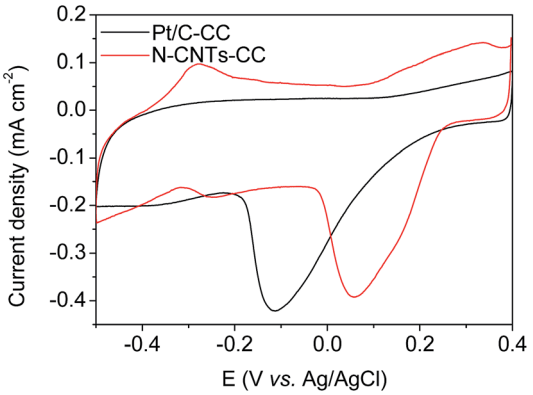

Fig. 6 CV of the Pt-cathode and N-CNT-cathode in a 50 mM phosphate buffer of pH 7.0, at the scan rate of 1 mV s^{-1}. Black line: Pt/C-CC; red line: N-CNT–CC.

results provided direct evidence for the smaller resistance of the N-CNT–CC electrode, resulting from the N-doping of the CNTs, which is beneficial to a smaller internal resistance of the MFC. Meanwhile, the N-doping of the CNTs also increased the activity sites of the electrode, and accordingly enhanced its ORR activity. Thus, the smaller resistance and the better ORR performance of the N-CNT–CC resulted in the higher power density of the MFC with the N-CNT–CC cathode.

In summary, we used a simple process to directly fabricate vertically-aligned N-CNTs on CC in this work, and used it as an efficient, low-cost cathode for an MFC. The N-CNT–CC electrode could increase the MFC power density by 8.6% compared to that with the Pt/C-CC electrode. The electrochemical characterization suggests that the better performance of the MFC with the N-CNT–CC cathode resulted from the smaller resistance and better ORR performance of the N-CNT–CC cathode. The present work provides an effective approach for preparing low-cost and efficient MFC cathodes, but further optimization of the electrode preparation process and conditions shall still be needed.

Acknowledgements

The authors wish to thank the National Natural Science Foundation of China (21477120 and 51538012), and the Program for Changjiang Scholars and Innovative Research Team in University and the Collaborative Innovation Center of Suzhou Nano Science and Technology of the Ministry of Education of China for the partial support of this work.

Notes and references

1 M. Zhu, C. Wang, D. Meng and G. Diao, *J. Mater. Chem. A*, 2013, **1**, 2118–2125.
2 Y. Q. Wang, H. Huang, B. Li and W. S. Li, *J. Mater. Chem. A*, 2015, **3**, 5110–5118.
3 J. Winfield, L. D. Chambers, J. Rossiter, J. Greenman and I. Ieropoulos, *J. Mater. Chem. A*, 2015, **3**, 7058–7065.
4 X. Chen, X. Wang, K. Liao, L. Zeng, L. Xing, X. Zhou, X. Zheng and W. Li, *J. Mater. Chem. A*, 2015, **3**, 19402–19409.

5 S. Oh, B. Min and B. E. Logan, *Environ. Sci. Technol.*, 2004, **38**, 4900–4904.
6 B. Kim, I. Chang and G. Gadd, *Appl. Microbiol. Biotechnol.*, 2007, **76**, 485–494.
7 X. W. Liu, X. F. Sun, Y. X. Huang, G. P. Sheng, K. Zhou, R. J. Zeng, F. Dong, S. G. Wang, A. W. Xu, Z. H. Tong and H. Q. Yu, *Water Res.*, 2010, **44**, 5298–5305.
8 D. Li, Y. Qu, J. Liu, W. He, H. Wang and Y. Feng, *J. Power Sources*, 2014, **272**, 909–914.
9 S. Zhong, L. Zhou, L. Wu, L. Tang, Q. He and J. Ahmed, *J. Power Sources*, 2014, **272**, 344–350.
10 Y. Yan, Y. Chen and L. Wang, *Energy Environ. Sci.*, 2011, **4**, 1892–1899.
11 Z. Liu, X. Fu, M. Li, F. Wang, Q. Wang, G. Kang and F. Peng, *J. Mater. Chem. A*, 2015, **3**, 3289–3293.
12 R. Zhang, S. He, Y. Lu and W. Chen, *J. Mater. Chem. A*, 2015, **3**, 3559–3567.
13 W. Zhao, P. Yuan, X. She, Y. Xia, S. Komarneni, K. Xi, Y. Che, X. Yao and D. Yang, *J. Mater. Chem. A*, 2015, **3**, 14188–14194.
14 J. Zhu, S. P. Jiang, R. Wang, K. Shi and P. K. Shen, *J. Mater. Chem. A*, 2014, **2**, 15448–15453.
15 C. Zhao, P. Gai, C. Liu, X. Wang, H. Xu, J. Zhang and J. J. Zhu, *J. Mater. Chem. A*, 2013, **1**, 12587–12594.
16 I. Kruusenberg, L. Matisen, H. Jiang, M. Huuppola, K. Kontturi and K. Tammeveski, *Electrochem. Commun.*, 2010, **12**, 920–923.
17 Z. Yang, H. Nie, X. A. Chen, X. Chen and S. Huang, *J. Power Sources*, 2013, **236**, 238–249.
18 R. Nie, X. Bo, C. Luhana, A. Nsabimana and L. Guo, *Int. J. Hydrogen Energy*, 2014, **39**, 12597–12603.
19 K. Gong, F. Du, Z. Xia, M. Durstock and L. Dai, *Science*, 2009, **323**, 760–764.
20 Y. Yao, B. Zhang, J. Shi and Q. Yang, *ACS Appl. Mater. Interfaces*, 2015, **7**, 7413–7420.
21 Z. Cui, S. Wang, Y. Zhang and M. Cao, *J. Power Sources*, 2014, **259**, 138–144.
22 W. Heming, W. Zhuangchun, A. Plaseied, P. Jenkins, L. Simpson, C. Engtrakul and R. Zhiyong, *J. Power Sources*, 2011, **196**, 7465–7469.
23 M. Ghasemi, M. Ismail, S. K. Kamarudin, K. Saeedfar, W. R. W. Daud, S. H. A. Hassan, L. Y. Heng, J. Alam and S. E. Oh, *Appl. Energy*, 2013, **102**, 1050–1056.
24 E. G. Rakov, *Russ. Chem. Rev.*, 2013, **82**, 538–566.
25 M. S. U. Sarwar, M. Dahmardeh, A. Nojeh and K. Takahata, *J. Mater. Process. Technol.*, 2014, **214**, 2537–2544.
26 B. Kim, H. Chung and W. Kim, *J. Phys. Chem. C*, 2010, **114**, 15223–15227.
27 S. Chen, J. Zhu and X. Wang, *J. Phys. Chem. C*, 2010, **114**, 11829–11834.
28 P. Sharma, V. Bhalla, V. Dravid, G. Shekhawat, E. S. Prasad and C. R. Suri, *Sci. Rep.*, 2012, **2**, 877.
29 S. Wang, E. Iyyamperumal, A. Roy, Y. Xue, D. Yu and L. Dai, *Angew. Chem., Int. Ed.*, 2011, **50**, 11756–11760.
30 A. E. Shalagina, Z. R. Ismagilov, O. Y. Podyacheva, R. I. Kvon and V. A. Ushakov, *Carbon*, 2007, **45**, 1808–1820.
31 S. Maldonado, S. Morin and K. J. Stevenson, *Carbon*, 2006, **44**, 1429–1437.
32 Y. R. He, X. Xiao, W. W. Li, G. P. Sheng, F. F. Yan, H. Q. Yu, H. Yuan and L. J. Wu, *Phys. Chem. Chem. Phys.*, 2012, **14**, 9966–9971.
33 C. He and P. K. Shen, *Electrochem. Commun.*, 2013, **35**, 80–83.
34 X. C. Abrevaya, N. J. Sacco, M. C. Bonetto, A. Hilding-Ohlsson and E. Cortón, *Biosens. Bioelectron.*, 2015, **63**, 580–590.
35 M. Ghasemi, M. Ismail, S. K. Kamarudin, K. Saeedfar, W. R. W. Daud, S. H. A. Hassan, L. Y. Heng, J. Alam and S. E. Oh, *Appl. Energy*, 2013, **102**, 1050–1056.
36 Y. Yan, B. Xia, Z. Xu and X. Wang, *ACS Catal.*, 2014, **4**, 1693–1705.
37 D. Yu, Y. Xue and L. Dai, *J. Phys. Chem. Lett.*, 2012, **3**, 2863–2870.
38 G. Wu, D. Li, C. Dai, D. Wang and N. Li, *Langmuir*, 2008, **24**, 3566–3575.

